A Novel Energy Partition for Gaining New Insight into Aromaticity and Conjugation

Zhong-Heng Yu,* Zheng-Qian Xuan, Tong-Xin Wang, and Hai-Min Yu

State Key Laboratory for Structural Chemistry of Unstable & Stable Species, Institute of Chemistry, Chinese Academy of Sciences, Beijing 100080, People's Republic of China

Received: August 24, 1999; In Final Form: November 19, 1999

To gain new insight into the nature of aromaticity and conjugation, we have developed a novel procedure for constructing a localized fragment molecular orbital basis set. It is a three-step procedure: (i) obtainment of each subcanonical FMO (fragment molecular orbital) basis set from a specific double bond fragment and its fragment molecule; (ii) the localization of the canonical FMOs; (iii) the superposition of all sublocalized FMO basis sets. On the basis of our procedure, Morokuma's energy partition provides, in the framework of ab initio SCF-MO computation at the STO-3G level, each of 46 compounds with various energy effects. The π-energy difference in each of four fictitious electronic states between the experimental and d_{SH} geometries shows that the delocalized π-system is practically destabilized. The π-system always prefers a distorted geometry. The role of the π-delocalization, stabilizing or destabilizing, depends on the response of the σ-framework to the π-delocalization. In the case of benzene-like and condensed-ring species, the vertical resonance energy (VRE) is always stabilizing. However, it is the σ-framework, rather than the π-system itself, that is strongly stabilized by the VRE. The energy effect $\Delta E_p^{(\pi)-\pi}$ of the π-delocalization on the π-system of the fragment itself is generally destabilizing, and it is found to be a Boltzmann model function of the net π charge transfer (CT) energy. The VRE of [N]annulene with $4N$ π-electrons is more destabilizing than that of [N]annulene with $4N + 2$ π electrons is stabilizing. It appears to be a prerequisite to the ring current that the π CT forms two closed circuits around the aromatic ring. In the case of benzene-like and condensed-ring compounds, the chemical shift is the Boltzmann model function of the net CT energy. As far as the VRE and chemical shift are concerned, the furan-like species appears not to be aromatic. However, the five-membered ring is the most rigid, and its hydrogen atom is a good leaving group, leading to high reactivity toward the substitution by an electrophilic reagent. The fact that $3H_2$ is more stable than regular hexagonal H_6 and its explanation imply that the delocalized σ-system is also destabilized.

1. Introduction

Aromaticity is arguably the most important general concept for the understanding of organic chemistry in general and of heterocyclic chemistry in particular. Since the isolation of benzene by Michael Farady in 1825, three criteria, such as geometric,[1] energetic,[2] and magnetic criteria,[3] are most widely used as quantitative measures of the degree of aromaticity.

Resonance energies, such as Hess−Schaad's resonance energy[2b] and Mulliken's vertical resonance energy,[4] are calculated on the basis of the approximations taking into account the π-electron subsystem only.

The concept of aromaticity is quantitative as well as qualitative, and many attempts have been made to define numerical scales or measures of aromaticity. Katritzky's principal component analysis gives the conclusions that the classical and magnetic concepts of aromaticity are almost completely orthogonal and there are at least two types of aromaticity.[5] Conversely, the linear relationships have been found existing between the magnetic susceptibility exaltation and aromatic stabilization energy,[6] between the ring current and resonance energy,[7] and even between chemical shift and chemical reactivity.[8] In this sense, the classical and magnetic criteria are not orthogonal.

The above-mentioned definitions and arguments are based on the conclusion that the molecule with $4N + 2$ π-electrons is π-aromatic. In the benzene case, it is the π-system that is strongly stabilized due to the delocalization of the π-electrons[9] (the phrase "the delocalization of the π-electrons" is shortened into "the π-delocalization" hereafter). Accordingly, the following questions arise: On one hand, why is benzene still reactive toward the electrophilic reagents? On the other hand, why is it much less reactive than thiophene although its aromatic energy (28.3 kcal/mol) is considerably larger than that (16.5 kcal/mol[2a]) of the latter?

The only answer to the questions seems to be that the delocalized π-system is destabilized. Whether the π-delocalization is stabilizing or not has been the subject of controversy.

Shaik and his collaborators argued that the delocalized π-system of benzene is not stable in the D_{6h} geometry, and delocalization of π-electrons is a byproduct of the σ-imposed geometric symmetry.[10] Shaik's viewpoint was supported by recent theoretical results: (i) the small degree of bond alternation in the distorted benzene ring of [4]paracyclophane, and the magnetic susceptibility of a boat-shaped benzene with the same geometry as [4]paracyclophane being the same as that of the hypothetical planar cyclohexatriene;[11] (ii) the small degree of bond alternation in the isomers of furanofuran and thienothiophene corresponding to less stability.[12]

* To whom correspondence should be addressed. E-mail: yuzh@infoc3.icas.ac.cn.

10.1021/jp993007f CCC: $19.00
Published on Web 02/24/2000

Recently, Epiotis criticized the concept of resonance stabilization vividly, and he argued that the right explanation of the remarkable benzene stability is the interpretation that the π aromatic system in benzene is less destabilized (rather than more stabilized) than alternative nonaromatic or antiaromatic species.[13a] It is possible for the viewpoint of resonance destabilization to gain the experimental ground. An important feature of furan chemistry is that electrophilic addition, as a side reaction in nitration with acetyl nitrate, occurs at the 2,5-positions rather than at the 2,3-positions.[14] In the 1970s, Jiang found the rule of homologous linearity of organic compounds from the UV of 150 homologous series of compounds. The rule reveals that in the compounds Ph−X (X = −OH, $-NH_2$), the resonance interaction between the group X and the phenyl ring is very weak.[15]

In the fictitious reference state with localized π double bonds, the density matrix elements d_{kl} between the p_z atomic orbitals are surely different from those in the same geometry with the full delocalized π-system. According to the following expression for the Fock matrix element.[16]

$$f_{ij} = h_{ij} + \sum_{m,n\neq p_z} d_{mn}[(ij, mn) - {}^1/_2(im, jn)] + \sum_{k,l}^{\text{all } p_z} d_{kl}[(ij, kl) - {}^1/_2(ik, jl)] \quad (1)$$

the π-delocalization should have an effect on the σ-framework through the space interaction. Our calculations[17] have shown that the role of the π-delocalization, stabilizing or destabilizing, depends upon the response of the σ-framework. In the case of the benzene molecule, it is the σ-framework, rather than the π-system itself, that is strongly stabilized by the vertical resonance energy (VRE). It reveals that benzene is σ-aromatic.[18]

In this work, our new procedure for constructing a localized fragment molecular orbital (FMO) basis set is described in detail. Morokuma's energy partition[19] is introduced into the intramolecular interaction, and it is used for analyzing, quantitatively, the direct and indirect effects of the π-delocalization on the π-system itself and the σ-frame in an effort to gain insight into the nature of the π-delocalization. Meanwhile, it is also applied to the σ-interaction to search for the unknown driving force. Our procedure will be utilized to evaluate the influence of the π-delocalization on the rigidity of the aromatic ring.

2. Method and Computational Detail

2.1. Morokuma Energy Partition. On the basis of the most common definitions, resonance energy is essentially associated with the local interaction between each pair of double bonds. Inevitably, this interaction influences the original characteristics of the double bonds, including the observed and calculable changes in their bond lengths and bond orders, and also including the disturbance to their original π-energies.[20] Accordingly, the fundamental problems in the energy partitioning are how to calculate, reasonably and directly, the π-energies occurring in a conjugated molecule and its reference state with the localized π-systems, and how to evaluate the effects of the π-delocalization on the π-systems themselves and the σ-framework. In this sense, the perturbation molecular orbital (PMO) theory should be more reasonable and valuable.

According to the PMO theory,[21] and on the basis of the definition of conjugation,[5] we can consider the benzene molecule, for example, as three ethylenic fragments, i.e., an A−B−C dissection as shown in Figure 1.

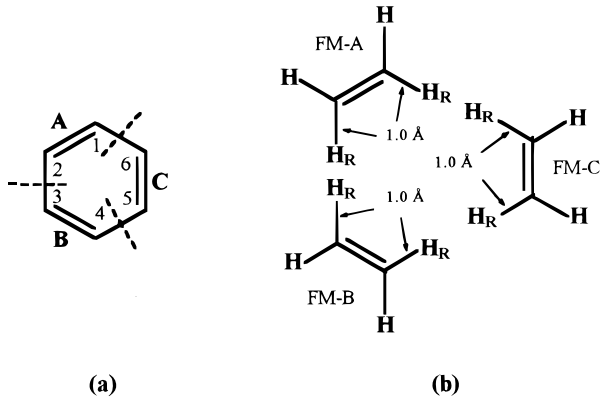

Figure 1. (a) A−B−C dissection of benzene into three ethylenic fragments, A, B, and C. (b) Formation of the corresponding fragment molecules FM-A, -B, and ,C. H_R is a referential hydrogen atom.

Figure 2 displays a thermodynamic cycle for the orbital interactions in two geometries of benzene. It shows the symbols for the π- and σ-electronic energies in the following fictitious states: the fully localized state (FUL), the DPI state with a delocalized π-system and localized σ-frameworks, the DSI state with a delocalized σ-framework and localized π-systems, and the fully delocalized state (FUD). Figure 2 also contains a set of definitions of various energy differences. For simplicity, these energy differences are expressed as the following general formulas:

$$\Delta E_\pi^{(\lambda,\rho)} = 0.5 \sum_{p\neq q}^{\text{all } p,q} \Delta E_{pq}^{(\lambda,\rho)-\pi} + \sum^{\text{all } p} \Delta E_p^{(\lambda,\rho)-\pi} \quad (2\text{-}1)$$

$$\Delta E_\sigma^{(\lambda,\rho)} = 0.5 \sum_{p\neq q}^{\text{all } p,q} \Delta E_{pq}^{(\lambda,\rho)-\sigma} + \sum^{\text{all } p} \Delta E_p^{(\lambda,\rho)-\sigma} \quad (2\text{-}2)$$

where $p, q = a, b, c, \ldots$, the characters λ and ρ ($\lambda, \rho = \pi, \sigma$) in the superscript ($\lambda, \rho$) mean that the energy effects $\Delta E_\pi^{(\lambda,\rho)}$ and $\Delta E_\sigma^{(\lambda,\rho)}$ arise from the delocalization of the λ- and ρ-electrons, and the characters π and σ in super- and subscripts denote that the energy effects are associated, respectively, with the π- and σ-orbital interactions. When $\lambda = \pi$ and $\rho = \sigma$, eqs 2-1 and 2-2 become

$$\Delta E_\pi^{\text{V}} = 0.5 \sum_{p\neq q}^{\text{all } p,q} \Delta E_{pq}^{\text{V}-\pi} + \sum^{\text{all } p} \Delta E_p^{\text{V}-\pi} \quad (3\text{-}1)$$

$$\Delta E_\sigma^{\text{V}} = 0.5 \sum_{p\neq q}^{\text{all } p,q} \Delta E_{pq}^{\text{V}-\sigma} + \sum^{\text{all } p} \Delta E_p^{\text{V}-\sigma} \quad (3\text{-}2)$$

where ΔE_π^{V} and $\Delta E_\sigma^{\text{V}}$ are the energy differences between the FUD and DSI states in the same geometry. Two terms on the right side of eq 3-1 are two energy components associated with the inter- and intrafragment interactions, respectively.

It should be particularly emphasized that the energy effect $\Delta E_\sigma^{\text{V}}$ in eq 3-2 is the response of the σ-framework to the π-delocalization, and it arises from the effect of the π-delocalization on the $\sigma-\pi$ space interactions expressed in terms of the Coulomb $J_{\sigma\pi}$ and exchange $K_{\sigma\pi}$ integrals. The local resonance interaction between carbon−carbon double bonds, i.e., the π-orbital interaction between fragments P and Q, and its effects on the π-system itself and the σ-framework are summarized in Scheme 1.

In the Morokuma energy partition, the energy components $E_p^{(\sigma)-\lambda}$ and $E_{pq}^{(\sigma)-\lambda}$ in the DSI state, for example, are obtained

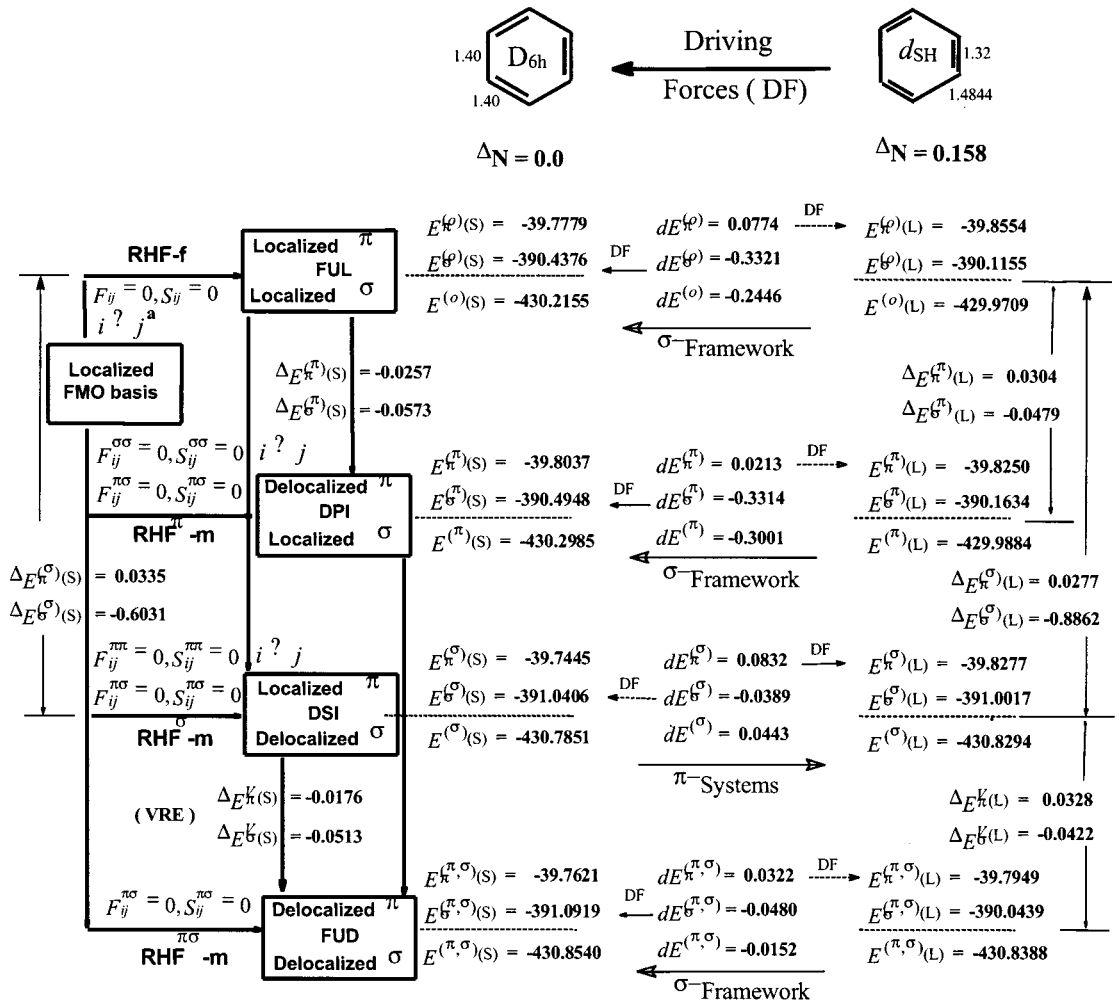

Figure 2. Thermodynamic cycle for the orbital interactions, the total electronic energy and its π- and σ-components, such as $E^{(\sigma)}$, $E_{\pi}^{(\sigma)}$, and $E_{\sigma}^{(\sigma)}$, in each of four electronic states denoted as FUL, DPI, DSI, and FUD, and the definitions of the various energy differences, such as $\Delta E_{\pi}^{(\sigma)}$ and $\Delta E_{\sigma}^{(\sigma)}$, between each pair of the electronic states in the same geometry and those, $dE^{(\sigma)}$, $dE_{\pi}^{(\sigma)}$, and $dE_{\sigma}^{(\sigma)}$, between the crystal structure of benzene and its d_{SH} geometry. Key: (a) $i \in$ P and $j \in$ Q when $i, j \in \pi$-systems; $i, j \in$ P and Q when $i, j \in \sigma$-frameworks.

SCHEME 1

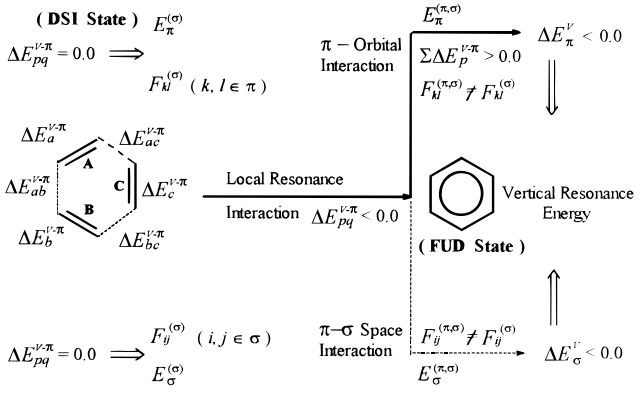

from the following general expressions:

$$E_{pq}^{(\sigma)-\lambda} = \sum_{i}^{\text{all }\lambda}\sum_{j}^{\text{all }\lambda}(F_{ij}^{(\sigma)} + H_{ij}^{(\sigma)})D_{ij}^{(\sigma)} \qquad i \in P, \quad j \in Q \qquad (4\text{-}1)$$

$$E_{p}^{(\sigma)-\lambda} = \sum_{i}^{\text{all }\lambda}\sum_{j}^{\text{all }\lambda}(F_{ij}^{(\sigma)} + H_{ij}^{(\sigma)})D_{ij}^{(\sigma)} \qquad i, j \in P \qquad (4\text{-}2)$$

where **F**, **H** and **D** are Fock, Hamiltonian, and density matrixes, respectively (a capital bold letter denotes, hereafter, a matrix over the localized FMO basis set). $F_{ij}^{(\sigma)}$, $H_{ij}^{(\sigma)}$, and $D_{ij}^{(\sigma)}$ are their respective elements in the DSI state.

Various elements in eqs.4-1 and 4-2 are obtained from the RHF (restricted Hartree−Fock) computation, denoted as RHF$^{\sigma}$-m in Figure 2, for the DSI state under the following conditions: in each SCF iteration, all the elements S_{ij} (the elements of the overlap integral matrix **S**) and F_{ij} ($i \in$ P, $j \in$ Q, and $i, j \in \pi$) are set equal to zero. The RHF$^{\pi\sigma}$-m computation for the elements $F_{ij}^{(\sigma,\pi)}$, $H_{ij}^{(\sigma,\pi)}$, and $D_{ij}^{(\sigma,\pi)}$ in the FUD state was performed under the constraint that all the F_{ij} and S_{ij} between the π and σ FMOs are set equal to zero. In the case of the planar molecule, it is a full RHF computation. In any case, the elements F_{ij} and S_{ij} between each of the pairs of the singly occupied FMOs are not equal to zero.

2.2. Construction of the Localized FMO Basis Set. The localized FMO basis set, in which all FMOs have correct electron occupancies, consists of the localized and singly occupied FMOs. The construction of this basis set is a three-step procedure: (i) obtainment of each subcanonical FMO basis set from a specific double bond fragment and its fragment molecule using Kost's localization followed by a conditional RHF computation;[22] (ii) transformation of the subcanonical FMOs into the localized FMOs employing Perkins' localization procedure;[23] (iii) formation of a localized FMO basis set for a

molecule by the superposition of all sublocalized FMO basis sets. The first step has been detailed elsewhere,[17] and it provides each fragment with a set of FMOs which are orthogonal and have correct orbital occupancies.

Perkins' localization procedure is based on the zero differential overlap. In the case of ab initio calculation, the overlap integrals $S_{ij} = \sum_{\rho\lambda} C_{\lambda i} C_{\rho j}$ in Perkins' procedure should be replaced with $S_{ij} = \sum_{\rho\lambda} C_{\lambda i} s_{\rho\lambda} C_{\rho j}$, where $s_{\rho\lambda}$ is the overlap integral between atomic orbitals ϕ_ρ and ϕ_λ. Perkins' localization concentrates the canonical FMOs on a single atom or two bonded atoms, leading to a set of localized FMOs that are approximately consistent with the standard description of the chemical bonds. Thus, the total σ electronic energy such as $E_\sigma^{(\sigma)}$ can also be partitioned into the contributions $\sum E_{CC}^{(\sigma)}$, $\sum E_{CH}^{(\sigma)}$, $\sum E_S^{(\sigma)}$ made by σ ring bonds, CH bonds, and various lone electron pairs according to the following expression:

$$E_\sigma^{(\sigma)} = \sum_{m,n}^{\text{CH bonds}} (F_{mn}^{(\sigma)} + H_{mn}^{(\sigma)}) D_{mn}^{(\sigma)} + \sum_{g,h}^{\text{ring bonds}} (F_{gh}^{(\sigma)} + H_{gh}^{(\sigma)}) D_{gh}^{(\sigma)} + \sum_{i,j}^{\text{all } S} (F_{ij}^{(\sigma)} + H_{ij}^{(\sigma)}) D_{ij}^{(\sigma)} + \sum_{k,l}^{\sigma} (F_{kl}^{(\sigma)} + H_{kl}^{(\sigma)}) D_{kl}^{(\sigma)} = \sum E_{CH}^{(\sigma)} + \sum E_{CC}^{(\sigma)}) + \sum E_S^{(\sigma)}) + \sum E_{kl}^{(\sigma)} \quad (5)$$

where the cross term $\sum E_{kl}^{(\sigma)}$ includes all other energy effects arising from the interactions between different types of chemical bonds.

3. Results and Discussion

The resonance energy is the energy difference between the real molecule and its fictitious reference state with localized π-electrons. Many efforts have been made to provide the reference state with a wave function.[4,24] However, our practical calculations have confirmed that the fundamental problem is how to calculate the Fock matrix in the reference state. In this sense, the DSI state obtained from our program is a reasonable and calculable reference state, and the corresponding resonance energy $\Delta E_\pi^V + \Delta E_\sigma^V$ is the so-called vertical resonance energy (Scheme 1).[4]

Comparison of the reports in the literature shows that the Gaussian-type basis sets have great influence on the VRE.[4b,c,24] In the case of *cis*-1,2-difluoroethylene, the destabilizing VRE (45.95 kcal/mol) from 4-31G is about 5 times as large as that (9.56 kcal/mol) from STO-3G.[21c]

The energy partition is based on analyzing the contributions of various FMOs to the total electronic energy. In *cis*-1,2-difluoroethylene, the overlap integral S_{na,π^*} is 0.134 (STO-3G) and 0.266 (4-31G).[21c] In the benzene case, the overlap integral between a pair of singly occupied FMOs is, for example, about 0.93 (4-31G to 6-311G) and 0.74 (STO-3G). Increasing the overlap integrals leads to overestimating the two π-electron stabilization energy ΔE_π^2 and the destabilization energy effect $\sum \Delta E_p^{V-\sigma}$, although the eventual total electronic energy from a larger basis is more accurate. Finally, only the STO-3G basis provides benzene with the stabilizing VRE (Table 1).

Owing to the fact that resonance is primarily a one-electron operator effect and on the basis of the literature result that electron correction reduces the calculation VRE of benzene by less than 10%, resonance energy can be, as indicated by Kollmar,[4b] well reproduced with a minimal basis and it is not very important to apply more flexible basis sets or even basis sets that include polarization functions. In this work, the localized FMO basis set and various energy effects were constructed and calculated using ab initio SCF-MO computation program at the STO-3G level.

TABLE 1: Overlap Integral S_{ij} between a Pair of Singly Occupied FMOs, the Effect $\sum \Delta E_p^{V-\sigma}$ of the π-Delocalization on the σ Intrafragment Interactions, the Total π Charge Transfer Energy ΔE_π^2, the Vertical Resonance Energy (VRE) and its Components ΔE_π^V and ΔE_σ^V Obtained from the RHF Computations for the FUD and DSI States of Benzene at the Four Gaussian-Type Basis Sets (Energy in hartrees)

	S_{ij}	$\sum \Delta E_p^{V-\sigma}$	ΔE_π^2	ΔE_π^V	ΔE_σ^V	VRE
STO-3G	0.73962	0.21150	−3.69598	−0.01763	−0.05128	−0.06891
4-31G	0.94035	1.42523	−4.17232	−0.38692	0.42296	0.03604
6-31G	0.93405	1.47544	−4.11789	−0.44745	0.49169	0.04424
6-311G	0.92122	1.79183	−3.98192	−0.58341	0.64266	0.05925

TABLE 2: Energy Effects $0.5\sum \Delta E_{pq}^{V-\pi}$ and $\sum \Delta E_p^{V-\pi}$ Associated with the Inter- and Intrafragment Interactions, the Vertical Resonance Energy (VRE) of Benzene-like Species, and Its Two Components ΔE_π^V and ΔE_σ^V (Energy in hartrees)

compound	ref	$0.5\sum \Delta E_{pq}^{V-\pi}$	$\sum \Delta E_p^{V-\pi}$	ΔE_π^V	ΔE_σ^V	VRE
benzene	25	−4.3437	4.3261	−0.0176	−0.0513	−0.0689
pyridine	26	−4.4504	4.4364	−0.0140	−0.0520	−0.0660
pyridazine	27	−3.8636	3.8620	−0.0016	−0.0537	−0.0553
pyrimidine	28	−4.5220	4.4888	−0.0332	−0.0418	−0.0750
pyrazine	29	−4.5350	4.5238	−0.0112	−0.0622	−0.0734
1,2,3-triazine	30	−4.5603	4.5115	−0.0488	−0.0345	−0.0833
1,2,4-triazine	30	−3.6578	3.6781	0.0203	−0.0718	−0.0515
1,3,5-triazine	31	−4.7224	4.6718	−0.0506	−0.0273	−0.0779
1,2,4,5-tetrazine	32	−4.6262	4.6022	−0.0240	−0.0596	−0.0836

3.1. Classification of Aromatic Compounds. In any one of the conjugated compounds, except for cyclobutadiene, listed in Tables 2−5, the local resonance interaction between fragments P and Q and its effect on the σ-framework, expressed in terms of $0.5\sum \Delta E_{pq}^{V-\pi}$ and ΔE_σ^V, respectively, are always stabilizing. On the contrary, the energy effect $\sum \Delta E_p^{V-\pi}$, arising from the effect of the π-delocalization on their original π-systems, is destabilizing. Accordingly, the aromatic compounds can be grouped into three types. The compounds with a six-membered ring, such as benzene, pyridine, and triazine, belong to the first type (benzene-like species). In each of these compounds, the energy gain $|0.5\sum \Delta E_{pq}^{V-\pi}|$ is greater than the energy loss $\sum \Delta E_p^{V-\pi}$. The π- and σ-systems are both stabilized due to the π-delocalization, and the VRE is stabilizing (Table 2). The second type refers to the condensed ring systems such as those listed in Table 3. In each of these compounds, the energy gain $|0.5\sum \Delta E_{pq}^{V-\pi}|$ becomes less than the energy loss $\sum \Delta E_p^{V-\pi}$, and the π-system itself is destabilized by the π-delocalization. However, the VRE is still stabilizing due to $|\Delta E_\sigma^V| > \Delta E_\pi^V$. The compounds with a five-membered ring (Table 4), such as furan, pyrrole, thiophene, and their isoelectronic derivatives, form the third type (furan-like species). In this type of molecule, the energy loss $\sum \Delta E_p^{V-\pi}$ is considerably larger than the energy gain $|0.5\sum \Delta E_{pq}^{V-\pi}|$. This leads to $|\Delta E_\sigma^V|$ being less than ΔE_π^V, and the eventual VRE becomes destabilizing.

It is interesting that the VRE of the planar [*N*]annulene and its component ΔE_σ^V, including their size and sign, change as the value of *N* increases (Table 5). The planar annulene with $N > 6$ is a theoretical molecule. The ΔE_π^V of [*N*]annulene is always destabilizing, and its value is monotonically increasing as the value of *N* increases. In the meantime the corresponding ΔE_σ^V is stabilizing when $N > 4$, and it strengthens wave upon wave. Consequently, the annulene with $4N$ π-electrons is, as expected by Epiotis in the 1970s,[21a] more antiaromatic than one with $4N + 2$ electrons is aromatic. The VRE of [8]annulene is,

TABLE 3: Energy Effects $0.5\sum\Delta E_{pq}^{V-\pi}$ and $\sum\Delta E_{p}^{V-\pi}$ Associated with the Inter- and Intrafragment Interactions, the Vertical Resonance Energy (VRE) of Condensed-Ring Compounds, and Its Two Components ΔE_{π}^{V} and ΔE_{σ}^{V} (Energy in hartrees)

compound	ref	$\sum\Delta E_{pq}^{V-\pi}$	$\sum\Delta E_{p}^{V-\pi}$	ΔE_{π}^{V}	ΔE_{σ}^{V}	VRE
naphthalene	33	−7.7379	7.8019	0.0640	−0.1401	−0.0761
2,7-naphthyridine	34	−7.6671	7.7298	0.0627	−0.1354	−0.0727
1,8-naphthyridine	35	−7.8651	7.9011	0.0360	−0.1128	−0.0768
quinoline	36a−c	−7.7257	7.7736	0.0479	−0.1204	−0.0725
phthalazine	37	−7.3656	7.4449	0.0793	−0.1387	−0.0594
pyrazino[2,3-*b*]pyrazine	38	−7.2469	7.2633	0.0164	−0.0890	−0.0726
indazole	39	−6.2306	6.4354	0.2048	−0.2117	−0.0069
indole	40	−6.0736	6.2804	0.2068	−0.2121	−0.0053
purine	41	−7.0879	7.1832	0.0953	−0.1260	−0.0307
1H-pyrrolo[2,3-*b*]pyridine	42	−7.5570	7.7459	0.1889	−0.2274	−0.0385
benzimidazole	43	−6.2112	6.3301	0.1189	−0.1326	−0.0137
anthracene	44	−12.7879	12.9058	0.1179	−0.2099	−0.0920
carbazole	45	−12.4112	12.6980	0.2868	−0.3656	−0.0788
acenaphthylene	46	−8.9814	9.0525	0.0711	−0.1236	−0.0525
phenathrene	47	−13.7367	13.7847	0.0480	−0.1647	−0.1167
pyrene	48	−18.4602	18.6321	0.1719	−0.3056	−0.1337

TABLE 4: Energy Effects $0.5\sum\Delta E_{pq}^{V-\pi}$ and $\sum\Delta E_{p}^{V-\pi}$ Associated with the Inter- and Intrafragment Interactions, the Vertical Resonance Energy (VRE) of Furan-like Species, and Its Two Components ΔE_{π}^{V} and ΔE_{σ}^{V} (Energy in hartrees)

compound	ref	$0.5\sum\Delta E_{pq}^{V-\pi}$	$\sum\Delta E_{p}^{V-\pi}$	ΔE_{π}^{V}	ΔE_{σ}^{V}	VRE
furan	49	−1.6160	1.9447	0.3287	−0.3078	0.0209
thiophene	50	−1.8081	2.0796	0.2715	−0.2607	0.0108
pyrrole	36c,d	−2.2338	2.4781	0.2443	−0.2225	0.0218
isoxazole	51	−1.7865	2.0685	0.2820	−0.2716	0.0104
oxazole	52	−1.7246	2.0247	0.3001	−0.2896	0.0105
1,2,5-oxadiazole	53	−1.5422	1.7882	0.2460	−0.2320	0.0140
1,3,4-oxadiazole	54	−1.6488	1.9065	0.2577	−0.2511	0.0066
pyrazole	55	−2.5194	2.7205	0.2011	−0.1832	0.0179
imidazole	56	−2.3300	2.5205	0.1905	−0.1701	0.0204
1,2,5-triazole	57	−2.1903	2.3920	0.2017	−0.1802	0.0215
1,2,4-triazole	58	−2.4591	2.5990	0.1399	−0.1305	0.0094
1,2,5-thiadiazole	59	−1.9960	2.2435	0.2475	−0.2375	0.0100
1,2,4- thiadiazole	60	−1.9527	2.1512	0.1985	−0.1954	0.0030
1,3,4- thiadiazole	61	−1.5981	1.7958	0.1977	−0.1982	−0.0001
1,2,3,4-tetrazole	62	−2.6230	2.7257	0.1027	−0.1073	−0.0046

TABLE 5: Energy Effects $0.5\sum\Delta E_{pq}^{V-\pi}$ and $\sum\Delta E_{p}^{V-\pi}$ Associated with the Inter- and Intrafragment Interactions, the Vertical Resonance Energy (VRE) of [*N*]Annulene, and Its Two Components ΔE_{π}^{V} and ΔE_{σ}^{V} (Energy in hartrees)

N	optimized goemetry	R_{long}	R_{short}	$0.5\sum\Delta E_{pq}^{V-\pi}$	$\sum\Delta E_{p}^{V-\pi}$	ΔE_{π}^{V}	ΔE_{σ}^{V}	VRE
4	HF/6-31G	1.51	1.37	0.6752	−0.6127	0.0625	0.0217	0.0842
8	AM1	1.442	1.335	−1.1466	1.1937	0.0471	−0.0163	0.0308
	MP2/6-31G**	1.471	1.351	−1.1060	1.1484	0.0424	−0.0182	0.0242
	HF/6-31G**	1.479	1.326	−0.9965	1.0405	0.0440	−0.0171	0.0269
10	AM1	1.405	1.352	−6.0849	6.1385	0.0536	**−0.0821**	**−0.0285**
	HF/6-31G**	1.431	1.356	−5.0796	5.1357	0.0561	−0.0777	−0.0216
12	AM1	1.430	1.335	−3.4196	3.4868	0.0672	−0.0565	0.0107
14	AM1	1.424	1.339	−6.0124	6.1007	0.0883	**−0.0946**	**−0.0063**
16	AM1	1.431	1.337	−5.5639	5.6578	0.0939	−0.0910	0.0029
16	HF/6-31G**	1.492	1.345	−4.2663	4.3525	0.0862	−0.0842	0.0020

for example, 19.33 kcal/mol, and that of its neighbor [10]-annulene is −17.88 kcal/mol.

3.2. π Charge Transfer. *3.2.1. The π System Is Destabilized Due to the π Charge Transfer.* Electron delocalization is an important concept in modern organic chemistry. The charge transfer (CT) arises from the two-electron interaction which mixes the occupied FMO of one fragment with the vacant FMO of the others and vice versa, and one of two exchange (EX) energies is associated with the four-electron interaction between the occupied FMOs. According to Morokuma's definitions,[19] these two interactions cause the π-delocalization between fragments P and Q.

The quantity ΔE_{ov}^{pq} is defined as the CT energy arising from the delocalization of the π-electrons from fragment P to fragment Q. Accordingly, the symbol dE_p^2 in eq 6−1 denotes the net charge transfer from all fragments Q to a specific fragment P ($P \neq Q$), and ΔE_p^2 in eq 6-2 is the corresponding total CT energy.

$$dE_p^2 = \sum_{p\neq q}^{\text{all } q}(\Delta E_{ov}^{qp} - \Delta E_{ov}^{pq}) = \sum_{p\neq q}^{\text{all } q} dE_{qp}^2 \qquad (6\text{-}1)$$

$$\Delta E_p^2 = \sum_{p\neq q}^{\text{all } q}(\Delta E_{ov}^{qp} + \Delta E_{ov}^{pq}) = \sum_{p\neq q}^{\text{all } q} \Delta E_{qp}^2 \qquad (6\text{-}2)$$

As mentioned previously, of three energy effects $0.5\sum\Delta E_{pq}^{V-\pi}$, $\sum\Delta E_{p}^{V-\pi}$ and ΔE_{σ}^{V}, only $\sum\Delta E_{p}^{V-\pi}$ resists delocalizing of the π-electrons, and it plays an important role in controlling the π-delocalization. To rationalize the effect of the

TABLE 6: Interfragment Interaction Energy $0.5\sum\Delta E_{pq}^{(\pi)-\pi}$, the Net Charge Transfer (CT) Energy dE_p^2 and Total CT Energy ΔE_p^2 between Fragment P and All Other Fragments Q, the Net π-Electron Charge D_p^π on Fragment P, and the Energy Loss $\Delta E_p^{(\pi)-\pi}$ of Fragment P (Energy in hartrees)

compound	$0.5\Delta\sum E_{pq}^{(\pi)-\pi}$	fragment	$\Delta E_p^{(\pi)-\pi}$	dE_p^2	ΔE_p^2	net charge D_p^π
benzene	−4.590 21	C_1═C_2 (A)	1.521 49	0.000 00	−2.544 42	0.000 00
		C_3═C_4 (B)	1.521 49	0.000 00	−2.544 42	0.000 00
		C_5═C_6 (C)	1.521 49	0.000 00	−2.544 42	0.000 00
pyrimidine	−4.634 13	N_1═C_2 (A)	1.377 15	−0.041 31	−2.611 51	−0.021 34
		N_3═C_4 (B)	1.757 41	0.114 30	−2.686 99	0.023 65
		C_5═C_6 (C)	1.471 90	−0.072 99	−2.557 52	−0.002 30
furan	−1.410 04	C_4═C_5 (C)	−0.772 11	−0.750 96	−1.347 33	−0.191 58
		C_2═C_3 (B)	0.289 22	−0.375 32	−1.324 62	−0.033 03
		O_1 (A)	2.150 93	1.126 29	−1.126 29	0.224 61
pyrrole	−1.776 81	C_4═C_5 (C)	−0.696 51	−0.814 69	−1.634 75	−0.207 15
		C_2═C_3 (B)	0.323 14	−0.512 22	−1.624 24	−0.054 27
		N_1H (A)	2.332 21	1.326 91	−1.326 91	0.261 42
thiophene	−1.816 47	C_4═C_5 (C)	−0.793 43	−0.793 82	−1.736 10	−0.212 70
		C_2═C_3 (B)	0.320 08	−0.437 04	−1.739 16	−0.063 24
		S_1 (A)	2.761 97	1.230 86	−1.230 86	0.275 95
1,2,3,4-tetrazole	−1.956 97	N_4═C_5 (C)	0.298 47	−0.620 26	−1.709 75	−0.066 54
		N_2═N_3 (B)	−0.793 37	−0.805 26	−1.588 64	−0.201 60
		N_1H (A)	2.519 37	1.425 51	−1.425 51	0.268 15

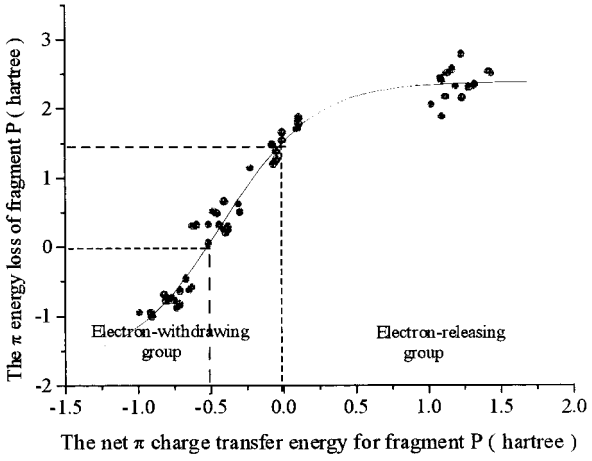

$$Y = [\ -4.095/(\ 1+ \exp((X + 0.4236)/0.3136)) + 2.3763\ ]$$

Figure 3. π energy loss (Y) $\Delta E_P^{(\pi)-\pi}$ of fragment P in the DPI state as the Boltzmann model function of the net π charge-transfer energy (X) dE_p^2.

π-delocalization on the π-system itself, the energy effects $0.5\sum\Delta - E_{pq}^{(\pi)-\pi}$, $\Delta E_p^{(\pi)-\pi}$, dE_p^2, and ΔE_p^2 and the net π-electron charge D_p^π on fragment P were calculated because the constrained conditions in the RHF computations for the FUL and DPI states ensure that the effect of the σ-delocalization on the π-systems has been eliminated as far as possible.

As shown by the data in Table 6, the π-system in an electron-releasing fragment with $dE_p^2 > 0.0$ is always destabilized due to the π-delocalization, and whether the π-system in an electron-withdrawing fragment is stabilized or not depends on the ratio of $|dE_p^2|$ to $|\Delta E_p^2|$. The statistical analysis formulates a Boltzmann model relationship, expressed in terms of $Y = -4.095/(1 + \exp((X + 0.4236)/0.3136)) + 2.3763$, between $\Delta E_p^{(\pi)-\pi}$ and dE_p^2 (Figure 3), and it shows that the energy loss $\Delta E_p^{(\pi)-\pi}$ increases as the net CT energy dE_p^2 becomes larger. In the pyrrole molecule, for example, the nitrogen fragment −NH− is a typical electron-releasing group. Its net CT energy dE_a^2 (1.327 hartrees), arising from the delocalization of the nitrogen lone pair into fragments B and C, is equal to the total CT energy $|\Delta E_a^2 = -1.327$ hartrees|, and the CT between fragments A and B as well as between A and C is unidirectional. As a result, its π-electron charge is +0.2614 and its energy loss $\Delta E_a^{(\pi)-\pi}$ is large, up to 2.33 hartrees. On the other hand, the net CT energy dE_c^2 for fragment C_4-C_5 is −0.8146 hartree and $|dE_c^2|/|\Delta E_c^2| = 0.50$. The ability of the fragment C_4-C_5 to withdraw π-electrons is so great that its $\Delta E_c^{(\pi)-\pi}$ (−0.6965 hartree) is stabilizing. However, the energy component $\sum\Delta E_p^{(\pi)-\pi}$ (1.959 hartrees), the energy effect $\Delta E_\pi^{(\pi)}$ (0.1820 hartree), and VRE (0.0488 hartree) are still destabilizing because the energy gains, including $\Delta E_c^{(\pi)-\pi}$ and $0.5\sum\Delta E_{pq}^{(\pi)-\pi}$, are insufficient to compensate for the π-energy loss $\Delta E_a^{(\pi)-\pi} + \Delta E_b^{(\pi)-\pi}$ (2.655 hartrees).

The above-mentioned theoretical results are well confirmed by the following radical reactions:

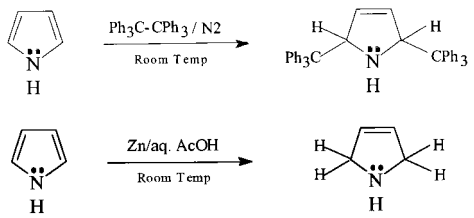

In these two reactions, the main products arise from 2,5-addition.[14]

3.2.2. π Charge Transfer and Chemical Shift. According to the Epiotis interpretation[13b] the ring current should depend on the π CT.

In Figure 4, a broken arrow indicates the direction of the CT between fragments P and Q, and a solid arrow denotes the orientation of the net CT. There is a fundamental difference in the CT between benzene- and furan-like species and cyclobutadiene. In benzene-like species, for example, each of two sets of the broken arrows forms a closed CT circuit around the aromatic ring.

Particularly, there is a corresponding relationship between the chemical shift δ (ppm)[8] and net CT energy dE_{pq}^2. Inspection of the orientations of the solid arrows in Figure 4 shows that there are two groups of aromatic compounds. In the first group of compounds, such as pyridine, pyrimidine, and triazine, three solid arrows point in the same direction, clockwise or anticlockwise. In the second group of compounds, such as pyrazine, pyridazine, and naphthalene, there are two counter-direction arrows pointing to two equivalent atoms. In the case of the second group of compounds, when the net CT energy, such as $dE_{ab}^2 = -0.0545$ hartree in pyrazine, is replaced with

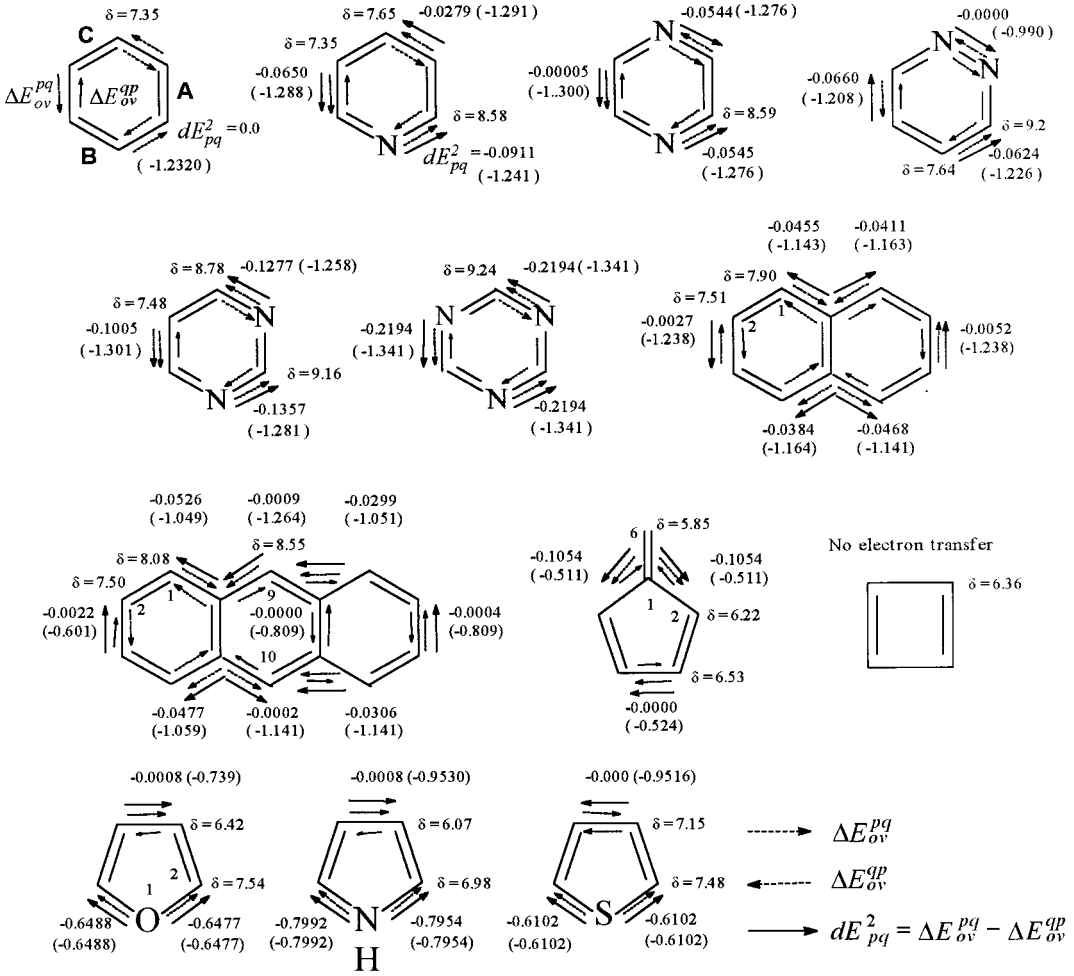

Figure 4. Net π charge transfer (CT) energy dE_{pq}^2 between fragments P and Q, and the experimental chemical shift δ (ppm). The number in parentheses is the total π CT energy $\Delta E_{pq}^2 = \Delta E_{ov}^{pq} + \Delta E_{ov}^{qp}$. The chemical shift of cyclobutadiene was calculated at the 6-31G** level using the Gaussian 98 program.

the sum $dE_{ab}^2 + dE_{ac}^2$ (−0.1089 hartree), the chemical shifts of the protons in the benzene-like species and naphthalene can be shown as a Boltzmann model function, expressed in terms of $Y = -1.824/(1 + \exp((X - 0.09372)/0.01974)) + 9.2704$, of the net CT energy dE_{pq}^2 (Figure 5).

On the other hand, there is no such closed CT circuit in furan-like species, fulvene and cyclobutadiene. The chemical shifts of the β-proton in furan as well as all the protons in pyrrole and fulvene are smaller than 7.0 ppm, and they are close to that of cyclobutadiene although the net CT energy dE_{ac}^2 in pyrrole is large, up to −0.799 hartree.

As far as the VRE and the chemical shift are concerned, furan-like species appear not to be aromatic. There should be unknown structural factors that make furan-like species reactive toward substitution by an electrophilic reagent. Lengthening of a double bond is a geometrical prerequisite for electrophilic addition. It is necessary to understand the driving force for distorting the aromatic ring.

3.3. The π-System Always Prefers a Distorted Geometry. To comprehend the driving force for distorting the aromatic ring and to analyze the effects of the π-delocalization on the direction and size of the driving force, the total π- and σ-electronic energies in the FUL, DPI, DSI, and FUD states and various energy differences (potential energies) between the crystal structure and its d_{SH} geometry were calculated.

The d_{SH} distortion was previously investigated by Shaik.[63] The d_{SH} geometry arises from variations in alternating the peripheral bond lengths within the constraint that the contribution of the nuclear repulsion to the total energy remains constant. In the d_{SH} geometry of benzene, the lengths of the shorter CC bonds were set equal to 1.32 Å. In this case, the aromatic index $\Delta N = \sum dN/n$, the average of the fluctuation of all the ring bonds,[64] for the d_{SH} geometry is larger than that for the crystal

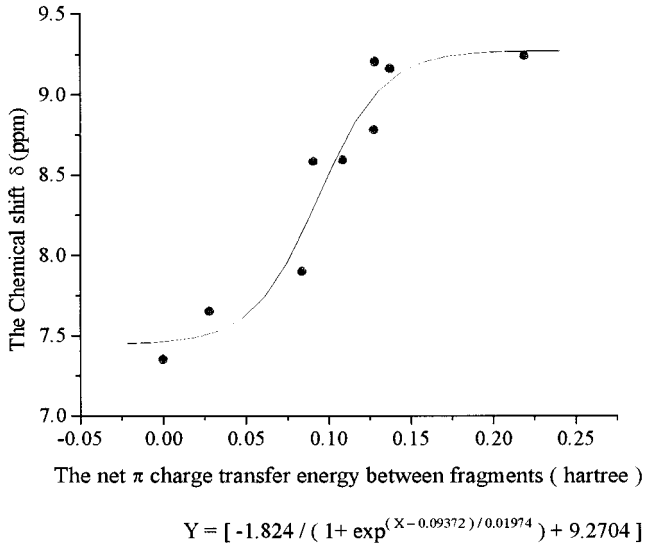

Figure 5. Chemical shift (Y) δ as the Boltzmann model function of the net π charge transfer energy (X) dE_{pq}^2 between fragments P and Q.

TABLE 7: Various Total Electronic Energies Obtained from the RHF Computations for the FUD and DSI States of Benzene at 4-31G, 6-31G, and 6-311G Basis Sets (Energy in hartrees)

	4-31G		6-31G		6-311G	
	D_{6h}	d_{SH}	D_{6h}	d_{SH}	D_{6h}	d_{SH}
			FUD State			
$E_\pi^{(\pi,\sigma)}$	−38.4075	−38.4824	−38.3263	−38.4056	−38.2025	−38.2882
$E_\sigma^{(\pi,\sigma)}$	−394.9324	−394.8398	−395.2611	−395.1630	−395.4232	−395.3199
$E^{(\pi,\sigma)}$	−433.3398	−433.3222	−433.5874	−433.5686	−433.6257	−433.6081
			DSI State			
$E_\pi^{(\sigma)}$	−38.0206	−38.2478	−37.8789	−38.1199	−37.6191	−37.8853
$E_\sigma^{(\sigma)}$	−395.3553	−395.1350	−395.7528	−395.5160	−396.0659	−395.8030
$E^{(\sigma)}$	−433.3759	−433.3828	−433.6317	−433.6359	−433.6850	−433.6883

structure. On the contrary, the d_{SH} geometries of furan and cyclobutadiene resulted from minimizing the difference in the CC bond lengths as far as possible. In this case, ΔN for the d_{SH} geometry is less than one for its corresponding optimized geometry. The characters L and S in the symbols such as $E_\pi^{(\sigma)}(L)$ and $E_\pi^{(\sigma)}(S)$ in Figures 2 and 6 denote the total electronic energies in the geometries with the larger and smaller ΔN.

3.3.1. Benzene. The role of the π-delocalization depends on the geometry of the benzene molecule. At the D_{6h} geometry (Figure 2), the π-delocalization always stabilizes the original π- and σ-systems, i.e., $\Delta E_\pi^{(\pi)}(S) < 0$, $\Delta E_\sigma^{(\pi)}(S) < 0$, $\Delta E_\pi^{V}(S) < 0$, and $\Delta E_\sigma^{V}(S) < 0$. The total electronic energy in the FUD state is the lowest. At the d_{SH} geometry, the delocalized π-systems in the FUD and DPI states become destabilized. The energy effects $\Delta E_\pi^{(\pi)}(L) = 19.08$ kcal/mol and $\Delta E_\pi^{V}(L) = 20.58$ kcal/mol and the total energy effects $\Delta E^{(\pi)}(L) = \Delta E_\pi^{(\pi)}(L) + \Delta E_\sigma^{(\pi)}(L)$ and $VRE(L) = \Delta E_\pi^{V}(L) + \Delta E_\sigma^{V}(L)$ are still stabilizing.

Comparison of the total π-electronic energies in the two geometries (Figure 2) shows that the delocalized π-system in the D_{6h} geometry is practically destabilized despite its $\Delta E_\pi^{(\pi)}(S) < 0$ and $\Delta E_\pi^{V}(S) < 0$. At the FUL state of the d_{SH} geometry, the total π-electronic energy $E_\pi^{(o)}(L)$ is −39.8554 hartrees, and it is the lowest of all the π-systems presented in Figure 2. The π potential energies $dE_\pi^{(o)}$, $dE_\pi^{(\pi)}$, $dE_\pi^{(\sigma)}$, and $dE_\pi^{(\pi,\sigma)}$ in the four

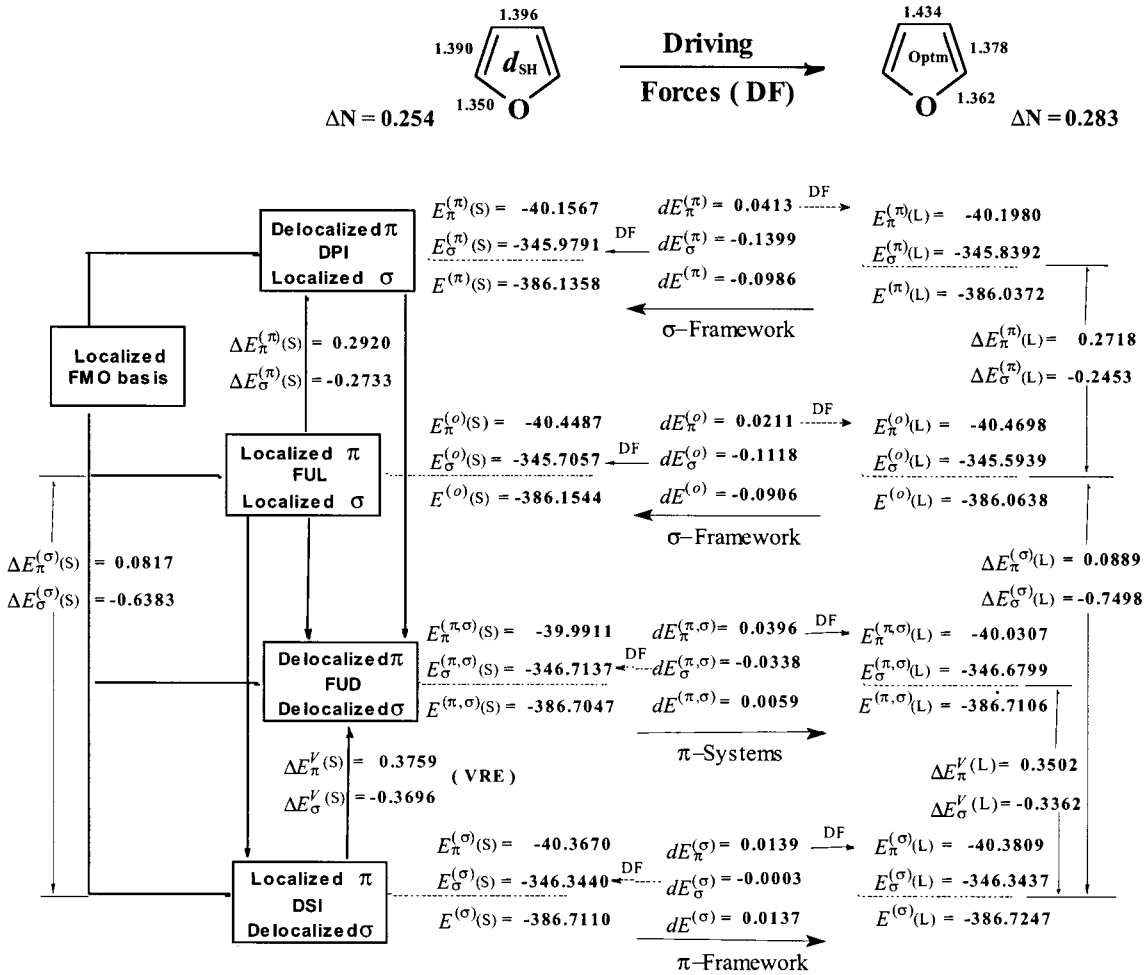

Figure 6. Thermodynamic cycle for the orbital interactions, the total electronic energy and its π- and σ-components in each of four electronic states denoted as FUL, DPI, DSI, and FUD and the various energy differences between each pair of electronic states in the same geometry and those between the optimized geometry of furan and its d_{SH} geometry. The optimized geometry was obtained from B3LYP/6-311G.

electronic states are all positive, and they are 48.57, 13.37, 52.21, and 20.21 kcal/mol, respectively. The π-system of benzene always prefers a distorted geometry no matter whether it is delocalized or not.

On the other hand, the values of the σ potential energy are always negative. In and only in the DSI state, the π potential energy is so large that $dE_\pi^{(\sigma)}$ (52.262 kcal/mol) > $|dE_\sigma^{(\sigma)}|$ (−24.359 kcal/mol). The total potential energy $dE^{(\sigma)} = E^{(\sigma)}(\mathrm{S}) - E^{(\sigma)}(\mathrm{L}) = dE_\sigma^{(\sigma)} + dE_\pi^{(\sigma)}$, i.e., the compression energy at constant nuclear repulsion, is about 28 kcal/mol, and it is close to Kollmar's compression energy (30 kcal/mol).[4b] The σ-framework in the DSI state only possesses a distortive tendency. It is the π-delocalization that makes this tendency become an effective driving force, expressed in terms of $dE_\sigma^{(\pi,\sigma)}$ (−30.1 kcal/mol) whose absolute value is now larger than that of $dE_\pi^{(\pi,\sigma)}$ (20.2 kcal/mol), for distorting a molecular structure with alternating long and short CC bond lengths to the D_{6h} geometry.

Various kinds of electronic energy obtained from the larger basis sets are listed in Table 7. The direction of the above-mentioned driving forces is not an artifact of a given basis. However, the Gaussian-type basis has a great influence on the size of the driving forces. The values of the compression energy at constant nuclear repulsion are, for example, about 4.33 (4-31G), 2.64 (6-31G), and 2.07 (6-311G) kcal/mol, which are much less than Kollmar's value. This is one more reason why the STO-3G basis set is more reasonable for Morokuma's energy partition. In fact, the STO-3G is accurate enough to calculate the energy difference. The difference in the total electronic energy $E^{(\pi,\sigma)}$ between D_{6h} and d_{SH} geometries is −0.0152 (STO-3G), −0.0176 (4-31G), −0.0188 (6-31G), and −0.0176 (6-311G) hartree.

3.3.2. Furan. It is a characteristic of furan-like species that both π potential energies $dE_\pi^{(\sigma)}$ (0.0139 hartree) and $dE_\pi^{(\pi,\sigma)}$ (0.0399 hartree) predominate over $dE_\sigma^{(\sigma)}$ (−0.0003 hartree) and $dE_\sigma^{(\pi,\sigma)}$ (−0.0338 hartree). At the FUD and DSI states, it is the π-system that distorts the molecule and its reference structure from the optimized geometry with $\Delta N = 0.254$ to one with $\Delta N = 0.283$ (Figure 6), and the σ-framework only possesses a tendency to level out of the differences in the bond length between the formal double and single bonds.

The following calculation results are particularly noteworthy: (i) the net driving force ($dE^{(\sigma)} = 0.0137$ hartree) in the DSI state is stronger than that ($dE^{(\pi,\sigma)} = 0.0059$ hartree) in the FUD states; (ii) the VRE (3.95 kcal/mol) in the d_{SH} geometry is less destabilizing than that (15 kcal/mol) in the optimized geometry. Keeping these in mind will help us to understand why furan-like species are aromatic and why $3H_2$ is more stable than regular hexagonal H_6.

3.3.3. Cyclobutadiene. The calculation results, $dE_\pi^{(\sigma)} = 0.0425$, $dE_{\mathrm{s}}{}^{(\sigma)} = -0.0437$, $dE_\pi^{(\pi,\sigma)} = 0.0691$, and $dE_\sigma^{(\pi,\sigma)} = -0.0392$ hartree, show a distinguished difference in the driving force between aromatic and antiaromatic compounds. In and only in the case of cyclobutadiene, $dE_\pi^{(\sigma)} < |dE_\sigma^{(\sigma)}|$ and $dE_\pi^{(\sigma)} > 0.0$. In the DSI state, an effective driving force arises from the σ-framework, and it distorts the optimized structure to the d_{SH} geometry with the smaller ΔN.

3.4. The Five-Membered Aromatic Ring Is the Most Rigid. A great number of the experimental data indicate that the π-delocalization always reduces the ionization potential.[15] In line with the experimental results, the eigenvalue of the highest occupied π MO in the FUD state is always larger than that in the DSI state (Table 8). The delocalized π-system should be more reactive toward electrophilic attack than the localized system as far as the charge transfer is concerned.

TABLE 8: Eigenvalues of the Highest Occupied π MOs in DSI and FUD States, the Contributions $\sum\Delta E_{\mathrm{CC}}^{\mathrm{V}}$ and $\Delta E_{\mathrm{CH}}^{\mathrm{V}}$ to $\Delta E_\sigma^{\mathrm{V}}$ Made by All σ Ring Bonds and a CH Bond, and the Component $E_{\mathrm{CH}}^{(\pi,\sigma)}$ of the Total σ-Electronic Energy $E_\sigma^{(\pi,\sigma)}$ in Each CH Bond

compounds	$e_{\mathrm{HOMO}}^{(\pi,\sigma)}$ (hartrees)	$e_{\mathrm{HOMO}}^{(\sigma)}$ (hartrees)	$\sum\Delta E_{\mathrm{CC}}^{\mathrm{V}}$ (kcal/mol)	$E_{\mathrm{CH}}^{(\pi,\sigma)}$ (hartrees)	$\Delta E_{\mathrm{CH}}^{\mathrm{V}}$ (kcal/mol)
pyrrole	−0.232 70	−0.342 98	−77.4975	−10.9177	30.6382
furan	−0.278 20	−0.381 04	−65.8258	−11.0272	28.2850
thiophen	−0.253 70	−0.293 43	3.3886	−12.2837	25.5083
imdazole	−0.266 91	−0.378 23	−54.5000	−11.2174	29.2545
oxazole	−0.301 30	−0.396 22	−63.3377	−11.1134	30.1343
isoxazole	−0.310 29	−0.393 75	−99.5764	−11.1376	15.5980
1,2,5-oxadiazole	−0.371 96	−0.409 54	−71.4351	−11.3761	19.5688
1,3,4-oxadiazole	−0.351 20	−0.410 31	−41.6999	−11.3224	34.1971
1,2,3,4-tetrazole	−0.360 20	−0.408 65	−72.0488	−11.6857	26.4056
benzene	−0.278 24	−0.331 63	12.8012	−11.7315	−6.1914
pyridine	−0.310 58	−0.340 85	21.7118	−12.3399	−7.0281
pyrazine	−0.334 77	−0.394 04	35.7053	−12.6127	−8.1419
pyrimidine	−0.340 61	−0.388 41	35.5171	−12.2976	−10.9030
pyridazine	−0.346 52	−0.388 76	40.3489	−12.4220	−6.6516
naphthalene	−0.237 10	−0.348 27	−18.3860	−15.3440	−5.3417
quinoline	−0.255 24	−0.347 89	−2.1963	−15.2104	−7.2253
cyclobutadiene	−0.218 14	−0.345 37	−4.9573	−9.3816	2.4002
[8]annulene	−0.190 78	−0.347 23	7.7811	−13.1722	−1.9217
[10]annulne	−0.227 05	−0.346 72	33.3207	−14.4638	−6.7018
[12]annulene	−0.184 67	−0.350 59	23.3433	−15.3756	−3.7075
[14]annulene	−0.210 76	−0.350 32	41.5411	−16.2131	−5.4773
[16]annulene	−0.181 85	−0.350 22	41.9804	−16.9334	−4.6710

Electrophilic attack gives the aromatic compound an intermediate cation while it distorts the aromatic ring. What happens next is determined by the relative activation energies, of deprotonation to give an aromatic compound and of simple nucleophilic addition to give a nonaromatic compound. As a mechanical property, the rigidity of the aromatic ring should be an important factor for determining the relative activation energy.

The aromaticity of three heterocycles, pyrrole, furan, and thiophene, is characterized by a very high degree of reactivity toward substitution by electrophilic reagents. Particularly, electrophilic attack occurs more readily at the α-position than at the β-position.[14] An important feature of furan-like species is, as previously mentioned, that electrophile addition occurs at the 2,5-positions rather than at the 2,3-positions. All these experimental results imply that the aromatic ring in furan-like species is much more rigid than the benzene ring.

According to eq 5, $\sum\Delta E_{\mathrm{CC}}^{\mathrm{V}}$ is the contribution to $\Delta E_\sigma^{\mathrm{V}}$ made by the whole peripheral σ-bond system, and it might be used to estimate the rigidity of the aromatic ring; $\Delta E_{\mathrm{CH}}^{\mathrm{V}}$ refers to an average component of $\Delta E_\sigma^{\mathrm{V}}$ in each C−H bond, and the contribution made by each CH bond to the total σ-electronic energy $E_\sigma^{(\pi,\sigma)}$ is denoted as $E_{\mathrm{CH}}^{(\pi,\sigma)}$. $\Delta E_{\mathrm{CH}}^{\mathrm{V}}$ and $E_{\mathrm{CH}}^{(\pi,\sigma)}$ appear to be able to scale the tendency to deprotonate.

There are fundamental and great differences in the sign and size of these three energy effects between furan- and benzene-like species and [*N*]annulene. Of all the compounds listed in Table 8, the furan-like species, except for thiophene, possess the most stabilizing $\Delta E_{\mathrm{CC}}^{\mathrm{V}}$ and the most destabilizing $\Delta E_{\mathrm{CH}}^{\mathrm{V}}$. Meanwhile, the values of their $E_{\mathrm{CH}}^{(\pi,\sigma)}$ are very close to that in benzene, and are much less than those in [*N*]annulene. The differences in $\Delta E_{\mathrm{CC}}^{\mathrm{V}}$ and $\Delta E_{\mathrm{CH}}^{\mathrm{V}}$ between pyrrole and benzene are, for example, large, up to −90.30 and 36.83 kcal/mol, respectively. These energy features, together with the characteristics of the driving forces, indicate that the heterocyclic ring in each of the furan-like species should be much more rigid

TABLE 9: Interaction Energy $0.5\sum\Delta E_{pq}^{(\sigma)}$ between Hydrogen Molecules, Its Components $\sum\Delta E_{pq}^{2}$ and $\sum\Delta E_{pq}^{4}$ Associated with the Two- and Four-Electron Interactions, the Energy Effect $\sum\Delta E_{p}^{(\sigma)}$, the Total Electronic Energies $E^{(o)}$ and $E^{(\sigma)}$ in the FUL and DSI States, and the Vertical Delocalization Energy (VDE) (Energy in hartrees)

d_{SH} (Å)	R_1 (Å)	$0.5\sum\Delta E_{pq}^{(\sigma)}$	$\sum\Delta E_{pq}^{2}$	$\Delta\sum E_{pq}^{4}$	$\sum\Delta E_{p}^{(\sigma)}$	$E^{(o)}$	$E^{(\sigma)}$	VDE
0.000	1.39	−1.169 28	−1.1101	0.0687	1.1919	−7.1102	−7.0876	0.0226
0.089	1.35	−0.851 38	−0.9149	0.1466	0.8961	−7.1370	−7.0922	0.0448
0.144	1.32	−0.637 95	−0.7683	0.1883	0.6942	−7.1577	−7.1016	0.0561
0.229	1.28	−0.405 53	−0.5913	0.2204	0.4701	−7.1859	−7.1212	0.0647
0.410	1.20	−0.116 32	−0.3286	0.2241	0.1821	−7.2442	−7.1784	0.0659
0.530	1.15	−0.024 01	−0.2206	0.2025	0.0840	−7.2815	−7.2216	0.0599
0.657	1.10	0.025 21	−0.1447	0.1727	0.0261	−7.3188	−7.2676	0.0513
0.938	1.00	0.050 28	−0.0567	0.1076	−0.0183	−7.3921	−7.3602	0.0320
1.270	0.90	0.033 83	−0.0185	0.0524	−0.0183	−7.4587	−7.4433	0.0154
1.688	0.80	0.012 70	−0.0044	0.0171	−0.0078	−7.5092	−7.5043	0.0049
2.000	0.742	0.004 96	−0.0015	0.0065	−0.0030	−7.5249	−7.5231	0.0018

SCHEME 2

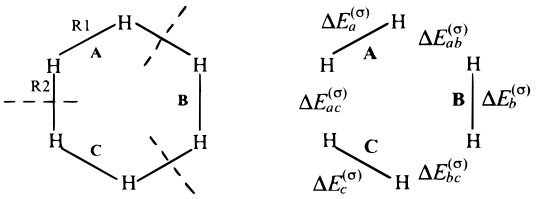

than the benzene ring, and its α-hydrogen is a good leaving group. Those may be the reasons why the addition product is eliminated greatly and it has to be replaced with the substitution product when the α-carbon is attacked. The furan-like species are still aromatic.

3.5. Regular Hexagonal H_6 Is Unstable Due to the σ-Electron Delocalization. In hexagonal H_6, there is no π-electron. It is necessary to explain why $3H_2$ is more stable than regular hexagonal H_6 (the phrase "hexagonal H_6" is often shortened into "H_6" hereafter) in light of our previous results.

In regular hexagonal H_6 and its various d_{SH} hexagons, three hydrogen molecules H_2 with the bond length R_1 (R_1 = 1.39−0.742 Å) are arranged in such a way (Scheme 2) that all H_6 molecules ($R_2 \geq R_1$, $d_{SH} = R_2 - R_1$) have the same nuclear repulsion energy. In the A−B−C dissection as shown in Scheme 2, breaking of the σ-bond is actually not involved. In this case, the sublocalized FMO basis for each fragment can be obtained directly from the full RHF computation for a hydrogen molecule with the bond length R_1. Then the localized FMO basis set for a specific H_6 is formed by the superposition of these three sublocalized FMO basis sets. The conditional and full RHF computations, over the localized FMO basis set, provide a specific H_6 with two electronic states, the FUL one with three isolated hydrogen molecules and the DSI one with a delocalized σ-framework. In the conditional RHF computation, all the elements S_{ij} and F_{ij} between hydrogen molecules are set equal to zero since there is no singly occupied FMO in the localized FMO basis set. Various energy effects and total electronic energies in each of 11 H_6 molecules are listed in Table 9. When d_{SH} = 2.0 Å and R_1 = 0.742 Å (an experimental value of hydrogen−hydrogen single bond length),[65] the distance (R_2 = 2.742 Å) between hydrogen molecules is so long that the total σ charge-transfer energy $\sum\Delta E_{pq}^{2}$ between hydrogen molecules decreases to −0.32 kcal/mol and the four-electron destabilization $\sum\Delta E_{pq}^{4}$ (1.36 kcal/mol) has predominated. In this case, H_6 can be practically considered as $3H_2$, and its entropy should be less than that of the corresponding free hydrogen molecules.

The energy effect $0.5\sum\Delta E_{pq}^{(\sigma)-\sigma}$, associated with the σ-electron interaction between hydrogen molecules, is stabilizing in the region of R_2 from 1.39 to 1.68 Å, and it is a Boltzmann function of d_{SH} (dashed line in Figure 7). Of all H_6 listed in Table 9, this energy effect is most stabilizing at the regular hexagon. Meanwhile, the energy effect $\sum\Delta E_{p}^{(\sigma)-\sigma}$, arising from the effect of the σ-delocalization on their original σ-frameworks, is destabilizing in the region of R_2 from 1.39 to 1.76 Å, and it is an exponential decay function of d_{SH} (solid line in Figure 7). The σ vertical delocalization energy (VDE) refers to the sum of $0.5\sum\Delta E_{pq}^{(\sigma)-\sigma}$ and $\sum\Delta E_{p}^{(\sigma)-\sigma}$, and it is always destabilizing (Figure 8). The maximum σ VDE (41.35 kcal/mol) occurs in the H_6 with d_{SH} = 0.410 Å. The σ VDE (14.18 kcal/mol) in regular hexagonal is much less destabilizing. As far as the VDE is concerned, regular hexagonal H_6 appears to be metastable.

When $VDE(d_{SH}) = E^{(\sigma)}(d_{SH}) - E^{(o)}(d_{SH})$ and the driving force $dE^{(\sigma)}(d_{SH}) = E^{(\sigma)}(d_{SH}) - E^{(\sigma)}(d_{SH} = 2.0) = dE^{(o)}(d_{SH}) +$ VDE-

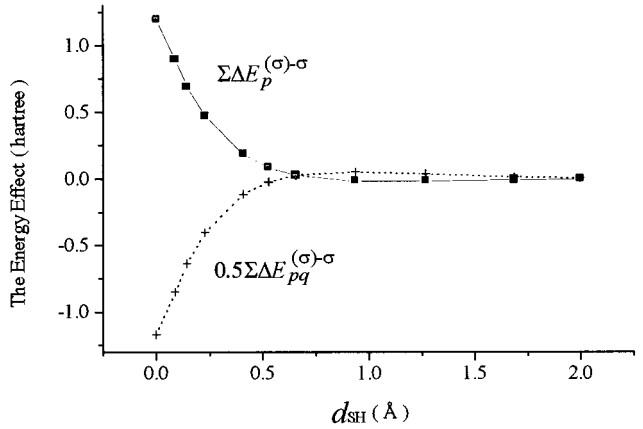

Figure 7. Energy effects $0.5\sum\Delta E_{pq}^{(\sigma)-\sigma}$ and $\sum\Delta E_{p}^{(\sigma)-\sigma}$ in hexagonal H_6 as Boltzmann (dashed line) and exponential decay (solid line) functions of d_{SH}.

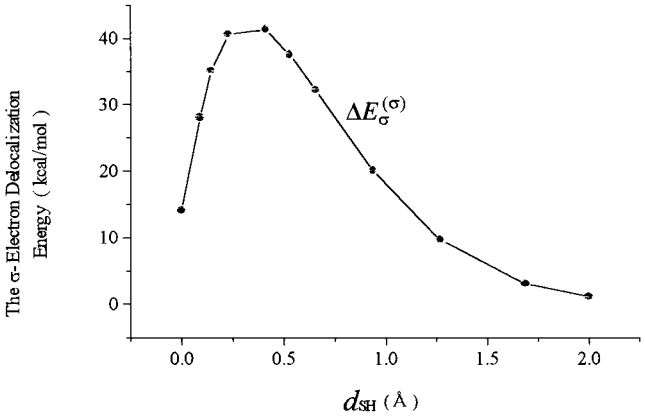

Figure 8. σ vertical delocalization energy $\Delta E_\sigma^{(\sigma)}$ in regular hexagonal H_6 and its d_{SH} hexagons.

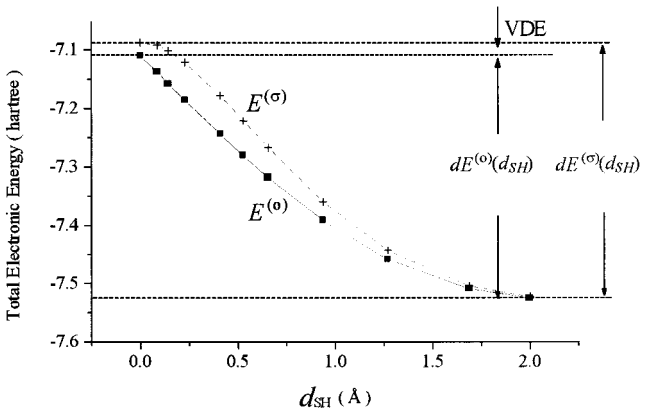

Figure 9. Total electronic energies $E_o^{(o)}$ and $E_\sigma^{(\sigma)}$ in the FUL and DSI states of hexagonal H_6 as an exponential decay (solid line) and a Lorentzian (dashed line) function of d_{SH}, respectively.

(d_{SH}) (see Figure 9), we can find that the VDE and the driving force for distorting H_6 from its regular hexagon to the D_{3h} one are two different physical quantities. The total electronic energy $E^{(o)}(d_{SH})$ in the FUL state is an exponential decay function of d_{SH} (solid line in Figure 9), and the total electronic energy $E^{(\sigma)}(d_{SH})$ in the DSI state is a Lorentzian function of d_{SH} (dashed line in Figure 9). Owing to the VDE(d_{SH}) > 0.0, the energy $E^{(\sigma)}(d_{SH})$ is always higher than its corresponding energy $E^{(o)}(d_{SH})$. Both driving forces $dE^{(\sigma)}(d_{SH})$ and $dE^{(o)}(d_{SH})$ distort the H_6 geometry from the regular hexagon to the hexagon with the largest possible d_{SH}, and the driving force $dE^{(\sigma)}(d_{SH})$ is greater than $dE^{(o)}(d_{SH})$.

It should be ascribed to the σ-delocalization that $3H_2$ is more stable than regular hexagonal H_6.

4. Summary

The Fock matrixes in various electronic states of an aromatic molecule are different. The construction of the localized FMO basis set for an actual molecule makes it possible to define a reference state precisely for calculating the vertical resonance energy.

Aromaticity does originate from the π-delocalization. However, we would argue that the role of the π-delocalization and its effect on the π-system itself are two very different concepts. To a great extent the method of transferring π charge between fragments determines the characters of an aromatic compound. The ring current, for example, should be ascribed to the π charge transfer that is able to form two closed circuits around the aromatic ring. Of three energy effects arising from the π-delocalization, only the energy effect $\sum\Delta E_p^{V-\pi}$ is destabilizing, and it plays an important role in controlling the delocalization of π-electrons and in classifying aromatic compounds. The ability of a specific fragment to resist delocalization of π-electrons depends on its capability to donate its π charge to all other fragments quantitatively. The π-system of an electron-releasing group, for example, is always strongly destabilized due to the π-delocalization. This is a fundamental reason why the delocalized π-system is practically destabilized, and why the π-system always prefers a distorted geometry. This is also the explanation why furan-like species appear not to be aromatic as far as the VRE is concerned. It should be especially emphasized that the space interaction between the π- and σ-systems has a great effect on the molecular behaviors. The Coulomb interaction is universal. The viewpoint that the π-delocalization is always stabilizing should be corrected.

Aromaticity has comprehended the thermodynamic, kinetic, and magnetic behaviors of aromatic compounds. Now it should include not only the effect of the π-delocalization on the π-system itself but also its influences on the σ-framework and various σ-bonds. Possibly a mechanical property such as the rigidity of the aromatic ring will be used as an additional criterion to measure the degree of aromaticity. Experiments to test the prediction about the VRE of furan-like species are underway.

The energy difference $\Delta E_\sigma^{(\sigma)}$ between the FUL and DSI states includes two energy effects, associated, respectively, with the σ-orbital interactions between fragments and the intrafragment interactions between the singly occupied and all other σ FMOs, and their effects on the original σ-framework. The orbital interactions resulting in electron delocalization should not include the intrafragment interaction. Hexagonal H_6 makes it possible to understand the nature of the σ-delocalization. The fact that $3H_2$ is more stable than regular hexagonal H_6 and its explanation imply that the σ-framework should also be destabilized due to the σ-delocalization.

Our energy partition at the STO-3G level will be a hopeful tool for analyzing the mechanism of the π charge transfer in a large molecule such as polynorbornylorous.

Acknowledgment. As one part of the State Key Basic Research and Development Plan (G1998010100), this work was supported by the Chinese government, National Natural Science Foundation of China (Grants 29872042 and 39890390), Special Foundation of the Chinese Academy of Sciences, and Research Foundation of the Director of the Institute of Chemistry, Chinese Academy of Sciences.

References and Notes

(1) Bergmann, E. D., Pullman, B., Eds. *Aromaticity, Pseudo-Aromaticity, Anti-Aromaticity*; Jerusalem Symposium on Quantitative Chemistry and Biochemistry; Israel Academy of Science and Humanities: Jerusalem, 1971; Vol. III.

(2) (a) Dewar, M. J. S.; Holder, A. J. *Heterocycles* **1989**, *28*, 1135. (b) Hess, B. S. A.; Schaad, L. S.; Holyoke, C. W. *Tetrahedron* **1975**, *31*, 295.

(3) (a) Dauben, H. J., Jr.; Wilson, J. D.; Laity, J. L. *J. Am. Chem. Soc.* **1968**, *90*, 811. (b) *Ibid.* **1969**, *91*, 1991.

(4) (a) Mulliken, R. S.; Parr, R. G. *J. Chem. Phys.* **1951**, *19*, 1271. (b) Kollmar, H. *J. Am. Chem. Soc*. **1979**, *101*, 4832. (c) Glendening, E. D.; Faust, R.; Streitwieser, A.; Vollhardt, K. P. C.; Weinhold, F. *J. Am. Chem. Soc*. **1993**, *115*, 10952.

(5) Katrizky, A. R.; Barczynski, P.; Musumarra, G.; Pisano, D.; Szafran, M. *J. Am. Chem. Soc*. **1989**, *111*, 7.

(6) (a) Von Raguè Schleyer, P.; Freeman P. K.; Jiao, H.; Goldfuss, B. *Angew. Chem., Int. Ed. Engl*. **1995**, *34*, 337. (b) Von Raguè Schleyer, P.; Jiao, H. *Pure Appl. Chem.* **1996**, *68*, 209.

(7) Haddon, R. C. *J. Am. Chem. Soc*. **1978**, *101*, 1722.

(8) Tamaoki, A.; Takahashi, K. *Bull. Chem. Soc. Jpn.* **1986**, *59*, 1650.

(9) (a) Streitweiser, A.; Heathcock, C. H. *Introduction to Organic Chemistry*; Macmillan: New York, 1985. (b) Neckers, D.; Doyle, M. P. *Organic Chemistry*; John Wiley: New York, 1977.

(10) (a) Shaik, S.; Hiberty, P. C.; Lefour, J. M.; Ohanessian, G. *J. Am. Chem. Soc.* **1987**, *109*, 363. (b) Hiberty, P. C.; Danovich, D.; Shurki, A.; Shaik, S. *J. Am. Chem. Soc*. **1995,** *117*, 7760.

(11) Sulzbach, H. M.; Remington, R. B.; Schaefer, H. F. *J. Am. Chem. Soc.* **1995**, *117*, 8392.

(12) Subramanian, G.; Von Raguè Schleyer, P.; Jiao, H. *Angew. Chem., Int. Ed. Engl*. **1996**, *35*, 2638.

(13) Epiotis, N. D. *Deciphering the Chemical Code*; VCH Publishers: New York, 1996; (a) p 267; (b) p 280.

(14) Joule, J. A.; Smith, G. F. *Heterocyclic Chemistry*; Van Nostrand Reinhold: London, 1972.

(15) Jiang, M. Q. *The Rule of Homologous linearity of Organic Compounds*; Science Press: Beijing, China, 1987 (English edition).

(16) Dewar, M. J. S. *The Molecular Orbital Theory of Organic Chemistry*; McGraw-Hill Books Inc.: New York, 1969.

(17) Yu, Z. H.; Li, L. T.; Fu, W.; Li, L. P. *J. Phys. Chem. A* **1998**, *102*, 2016.

(18) (a) Epiotis, N. D. *Pure Appl. Chem.* **1983**, *55*, 29. (b) Epiotis, N. D. *Lecture Notes in Chemistry*; Springer-Verlag: New York, 1983; Vol. 34, p 360.

(19) Kitaura, K.; Morokuma, K. *Int. J. Quantum Chem.* **1976**, *10*, 325.

(20) Libit, L.; Hoffmann, R. *J. Am. Chem. Soc.* **1974**, *96*, 1370.
(21) (a) Epiotis, N. D.; Cherry, W. R.; Shaik, S.; Yates, R.; Bernardi, F. *Topics in Current Chemistry*; Springer: New York, 1977; Vol. 70, p 27. (b) Dewar, M. J. S.; Dougherty, R. C. *The PMO Theory of Organic Chemistry*; Plenum Press: New York and London, 1975. (c) Bernardi, F.; Bottoai, A.; Epiotis, N. D.; Guerra, M. *J. Am. Chem. Soc.* **1978**, *100*, 6018.
(22) (a) Kost, D.; Schlegel, H. B.; Mitchell, D. J.; Wolfe, S. *Can. J. Chem.* **1979**, *57*, 729. (b) Yu, Z. H. *Comput. Chem.* **1994**, *18*, 95.
(23) (a) Perkins, P. G.; Stewart, A. J. P. *J. Chem. Soc., Faraday Trans 2* **1982**, *78*, 285. (b) Stewart, J, J. P. MOPAC, Version 6, Frank J. Seiler Research Laboratory, United States Air Force Academy, 1990.
(24) Behrens, S.; Köster, A. M.; Jug, K. *J. Org. Chem.* **1994**, *59*, 2546.
(25) André, D.; Renaud, M. *Acta Crystallogr.* **1971**, *B27*, 1275.
(26) Mootz, D.; Wussow, H. G. *J. Chem. Phys.* **1981**, *75* (3), 1517.
(27) Blake, A. J.; Rankin D. W. H. *Acta Crystallogr.* **1991**, *C47*, 1933.
(28) Wheatley, P. J. *Acta Crystallogr.* **1960**, *13*, 80.
(29) De With, G.; Harkema S.; Feil D. *Acta Crystallogr.* **1976**, *B32*, 3178.
(30) Mó, O.; De Paz, J. L. G.; Yáñez, M. *THEOCHEM* **1987**, *150*, 135.
(31) Wheatley, P. J. *Acta Crystallogr.* **1955**, *8*, 224.
(32) Bertinotti, F.; Giacomello, G.; Liquori, A. M. *Acta Crystallogr.* **1956**, *9*, 510.
(33) Brock, C. P.; Dunitz, J. D. *Acta Crystallogr.* **1982**, *B38*, 2218.
(34) Huiszoon, C.; Van Hummel, G. J.; Van Den Ham D. M. W. *Acta Crystallogr.* **1977**, *B33*, 1867.
(35) Clearfield, A.; Sims, M. J.; Singh P. *Acta Crystallogr.* **1972**, *B28*, 350.
(36) (a) Folting, K.; Merritt Jr, L. L. *Acta Crystallogr.* **1977**, *B33*, 3540. (b) Lenner, M.; Lindgren, O. *Acta Crystallogr.* **1976**, *B32*, 1903. (c) Tai, J. C.; Yang, L.; Allinger, N. L. *J. Am. Chem. Soc.* **1993**, *115*, 11906. (d) Nygaard L.; Nielsen J. T.; Kirchheiner J.; Maltesen G.; Rastrup-Andersen J.; Sørensen G. O. *J. Mol. Struct.* **1969**, *3*, 491.
(37) Huiszoon, C.; Van De Waal, B. W.; Van Egmond, A. B.; Harkema, S. *Acta Crystallogr.* **1972**, *B28*, 3415.
(38) Robey M. J.; Sterns M.; Morris H. M.; Ross, I. G. *J. Cryst. Mol. Struct.* **1971**, *1*, 401.
(39) Escande, P. A.; Lapasset J. *Acta Crystallogr.* **1974**, *B30*, 2009.
(40) Caminati, W.; Di Bernardo, S. *J. Mol. Spectrosc.* **1990**, *240*, 253.
(41) Watson, D. G. *Acta Crystallogr.* **1965**, *19*, 573.
(42) Dufour, P.; Dartiguenave, Y.; Dartiguenave, M.; Dufour, N.; Lebuis, A.; Bélanger-Gariépy, F.; Beauchamp, A. L. *Can. J. Chem.* **1990**, *68* (1), 193.
(43) Velino, B.; Trombetti, A.; Cané, E. *J. Mol. Spectrosc.* **1992**, *152*, 434.
(44) Brock, C. P.; Dunitz, J. D. *Acta Crystallogr.* **1990**, *B46*, 795.
(45) Kurahashi, M.; Fukuyo, M.; Shimada, A.; Furusaki, A.; Nitta, I. *Bull. Chem. Soc. Jpn.* **1968**, *42*, 2174.
(46) Wood, R. A.; Welberry, T. R.; Rae, A. D. *J. Chem. Soc., Perkin Trans. 2* **1985**, 451.
(47) Kay, M. I.; Okaya, Y.; Cox, D. E. *Acta Crystallogr.* **1971**, *B27*, 26.
(48) Hazell, A. C.; Larsen, F. K.; Lehmann, M. S. *Acta Crystallogr.* **1972**, *B28*, 2977.
(49) Fourme, P. R. *Acta Crystallogr.* **1972**, *B28*, 2984.
(50) Bak, B.; Christensen, D.; Hansen-Nygaard, L.; Rastrup-Andersen, J. *J. Mol. Spectrosc.* **1961**, *7*, 58.
(51) Stiefvater, O. L. *J. Chem. Phys.* **1975**, *63(6)*, 2560.
(52) Kumar, A.; Sheridan, J.; Stiefvater, O. L. *Z. Naturforsch.* **1978**, *33a*, 145.
(53) Stiefvater, O. L. *Z. Naturforsch.* **1988**, *43a*, 597.
(54) Nygaard, L.; Hansen, R. L.; Nielsen, J. T.; Rastrup-Andersen, J.; Sorensen, G. O.; Steiner P. A. *J. Mol. Struct.* **1972**, *12*, 59.
(55) Berthou, P. J.; Elguero, J.; Rérat, C. *Acta Crystallogr.* **1970**, *B26*, 1880.
(56) McMullan, R. K. *Acta Crystallogr.* **1979**, *B35*, 688.
(57) Begtrup, M.; Nielsen, C. J.; Nygaard, L.; Samdal, S. Sjogren, C. E.; Sorensen, G. O. *Acta Chem. Scand.* **1988**, *A42*, 500.
(58) Jeffrey, G. A.; Ruble, J. R.; Yates, J. H. *Acta Crystallogr.* **1983**, *B39*, 388.
(59) Stiefvater, O. L. *Z. Naturforsch.* **1978**, *33a*, 1511.
(60) Stiefvater, O. L. *Z. Naturforsch.* **1976**, *31a*, 1681.
(61) La Cour, T. *Acta Crystallogr.* **1974**, *B30*, 1642.
(62) van der Putten, N.; Heijdenrijk, D.; Schenk, H. *Cryst. Struct. Commun.* **1974**, *3*, 321.
(63) Shaik, S.; Hiberty, P. C.; Lefour, J. M.; Ohanessian, G. J. *J. Am. Chem. Soc.* **1987**, *109*, 363.
(64) Pozharskii, A. F. *Chem. Heterocycl. Compd.* **1985**, *21*, 717.
(65) Levine, I. N. *Quantum Chemistry*; Allyn and Bacon Inc.: Boston, 1975.